J. Astrophys. Astr. (December 2017) 38:66
https://doi.org/10.1007/s12036-017-9489-y

Quasinormal Modes of a Quantum-Corrected Schwarzschild Black Hole for Electromagnetic Perturbation

CHUNYAN WANG[1,2,*], YAJUN GAO[2], WENBO DING[2] and QINGXU YU[1]

[1]School of Physics and Optoelectronic Technology, Dalian University of Technology, Dalian 116024, People's Republic of China.
[2]Department of Physics, School of Mathematics and Physics, Bohai University, Jinzhou 121013, People's Republic of China.
*Corresponding author. E-mail: loveyan-zi@126.com

MS received 19 April 2017; accepted 11 October 2017; published online 27 November 2017

Abstract. In this work, we investigate the electromagnetic perturbation around a quantum-corrected Schwarzschild black hole. The complex frequencies of the quasinormal modes are evaluated by the third-order WKB approximation. The numerical results obtained showed that the complex frequencies depend on the quantum correction parameter a of a black hole, which the real parts and the magnitudes of the imaginary parts of quasinormal modes decrease with the increase in factor a. These conclusions show that the electromagnetic perturbation around the black hole oscillate and damp more slowly owing to the presence of the quantum correction parameter.

Keywords. Electromagnetic perturbation—quasinormal modes frequencies—WKB approximation.

1. Introduction

It is well known that the dynamical evolution of field perturbation on a black hole consists of roughly three stages (Frolov & Novikov 1998). The first one is an initial wave burst coming directly from the source of perturbation and is dependent on the initial form of the original wave field. The second one involves the damped oscillations named as quasinormal modes (QNMs), which are dependent only on the structure of the background spacetime and independent of the initial perturbation. The last one is a power-law tail behavior of the waves at a very late time which is caused by back scattering of the gravitational field.

The concept of quasinormal modes was first put forth by Vishweshwara (1970). It is widely believed that the QNMs in the dynamical evolution carry the unique characteristic information which lead to the direct identification of the black hole existence in our Universe or not. One can extract information about the physical parameters (mass, electric charge and angular momentum) of a black hole from the gravitational wave signal and test the stability of the event horizon against small perturbations (Chandrasekhar & Detweiler 1975; Chandrasekhar 1983; Kokkotas & Schmidt 1999). Different fields of perturbation (added as a test field, but does not take into account for construction of the background equilibrium model) in the geometry of a black hole can excite certain combination of its characteristic frequencies, a great deal of work has been studied (Regge & Wheeler 1957; Cardoso & Lemos 2001, 2003; Nollert 1993, 1999; Kunstatter 2003; Berti *et al.* 2004; Berti & Cardoso 2006; Konoplya 2002, 2005; Jing 2004; Jing & Pan 2005; Shu & Shen 2004; Giammatteo & Moss 2005; Chen & Jing 2013).

In 1994, Kazakov and Solodukhin gave a new expression of the Schwarzschild metric when the back reaction of the spacetime due to quantum fluctuations is taken into account (Kazakov & Solodukhin 1994). It is well known that the quantum vacuum fluctuations modify the geometry of the original Schwarzschild black hole, while the different geometry structure will lead to many new physical phenomenon and conclusions. More recently, the QNMs of scalar field perturbation around a quantum-corrected Schwarzschild black hole showed that the scalar field damps more slowly and oscillates more slowly due to the quantum fluctuations (Mahamat *et al.* 2014), and then the gravitational and

Dirac field perturbation have also been discussed, and conclusion obtained is that quasinormal modes of gravitational and Dirac perturbations of the Schwarzschild black hole damp more slowly and oscillate more slowly due to the quantum fluctuations (Mahamat *et al.* 2016). In this work, we are interested in studying the behavior of electromagnetic perturbation around this black hole.

In section 2, the metric of the quantum-corrected Schwarzschild black hole and the wave equation of electromagnetic perturbation are given. In section 3, we calculate the quasinormal frequencies by using the third-order WKB approximation and the results are presented using tables and figures. The summary is presented in the last section.

2. The metric and electromagnetic perturbation

The background metric of the quantum deformation of the Schwarzschild black hole is defined by (Kazakov & Solodukhin 1994)

$$\mathrm{d}s^2 = f(r)\mathrm{d}t^2 - f(r)^{-1}\mathrm{d}r^2 - r^2(\mathrm{d}\theta^2 + \sin^2\theta\mathrm{d}\varphi^2) \tag{1}$$

and the metric coefficient

$$f(r) = -\frac{2M}{r} + \frac{1}{r}\int^r U(\rho)\mathrm{d}\rho, \tag{2}$$

where M is the black hole mass. For the empty space, $U(\rho) = 1$, the metric can easily be reduced to the Schwarzschild black hole solution.

When taking into account the quantum fluctuation of vacuum (Wontae & Yongwan 2012), the quantity $U(\rho)$ transforms to

$$U(\rho) = \mathrm{e}^{-\rho}\left[\mathrm{e}^{-2\rho} - \frac{4}{\pi}G_\mathrm{R}\right]^{-1/2}, \tag{3}$$

where $G_\mathrm{R} = G_\mathrm{N}\ln(\mu/\mu_0)$, G_N is the Newton constant and μ is a scale parameter satisfying $t = \ln\frac{\mu}{\mu_0}$, while $\mu = \mu_0$ for $t = 0$ (Kazakov & Solodukhin 1994). The metric coefficient equation (2) can be read as

$$f(r) = \frac{1}{r}[-2M + \sqrt{r^2 - a^2}], \tag{4}$$

where the quantum correction parameter a has the dimensionality of length and $a^2 = 4G_\mathrm{R}/\pi$. Here, the scalar curvature of the spacetime does not depend on the mass of the gravitating body but depends on the quantum correction parameter.

For $r \gg a$, the metric coefficient becomes

$$f(r) \simeq 1 - \frac{2M}{r} - \frac{a^2}{2r^2} \tag{5}$$

which looks like the metric of a charged body with mass and imaginary charge $\pm i\frac{a}{\sqrt{2}}$. Thus, we can say that the quantum correction parameter a acts as an imaginary charge added to the spacetime metric. The metric (5) looks asymptotically like a Reissner–Nordström metric but with an imaginary electric charge. It will give a completely different behavior of quasinormal modes with electromagnetic perturbation because of the negative signature of the third term in the metric (5).

We consider the evolution of a Maxwell field in this spacetime. And the evolution is given by Maxwell's equations

$$F^{\mu\nu}_{;\nu} = 0, \quad F_{\mu\nu} = A_{\nu,\mu} - A_{\mu,\nu}, \tag{6}$$

where $F_{\mu\nu}$ is the electromagnetic tensor, and A_μ is the electromagnetic vector potential. In this background equation (1), one can expand A_μ in four-dimensional vector spherical harmonics (Ruffini 1973)

$$A_\mu(t,r,\theta,\varphi) = \sum_{l,m}\left(\begin{bmatrix} 0 \\ 0 \\ \frac{a^{lm}(t,r)}{\sin\theta}\partial_\varphi Y_{lm} \\ -a^{lm}(t,r)\sin\theta\,\partial_\theta Y_{lm} \end{bmatrix} + \begin{bmatrix} j^{lm}(t,r)Y_{lm} \\ h^{lm}(t,r)Y_{lm} \\ k^{lm}(t,r)\partial_\theta Y_{lm} \\ k^{lm}(t,r)\partial_\varphi Y_{lm} \end{bmatrix}\right), \tag{7}$$

where the first term in the right side has parity $(-1)^{l+1}$ and and the second term has parity $(-1)^l$, l is the angular quantum number and m is the azimuthal number.

Adopting the following form

$$\begin{aligned} a^{lm}(t,r) &= a^{lm}(r)\mathrm{e}^{-i\omega t}, \quad j^{lm}(t,r) = j^{lm}(r)\mathrm{e}^{-i\omega t}, \\ h^{lm}(t,r) &= h^{lm}(r)\mathrm{e}^{-i\omega t}, \quad k^{lm}(t,r) = k^{lm}(r)\mathrm{e}^{-i\omega t} \end{aligned} \tag{8}$$

and then submitting the expansion (7) into the Maxwell equation (6), with the tortoise coordinate r_* satisfying $\mathrm{d}r_* = \frac{\mathrm{d}r}{f(r)}$, we can obtain a second order differential equation for the perturbation

$$\frac{\mathrm{d}^2\Psi(r)}{\mathrm{d}r_*^2} + [\omega^2 - V(r)]\Psi(r) = 0. \tag{9}$$

The wavefunction $\Psi(r)$ is a linear combination of the functions a^{lm}, j^{lm}, h^{lm} and k^{lm}. The form of wavefunction depends on the parity of the perturbation. And the effective potential $V(r)$ can be expressed as

$$V(r) = f(r)\frac{l(l+1)}{r^2} \tag{10}$$

when the metric is (4), we will evaluate quasinormal modes of quantum-deformed Schwarzschild black

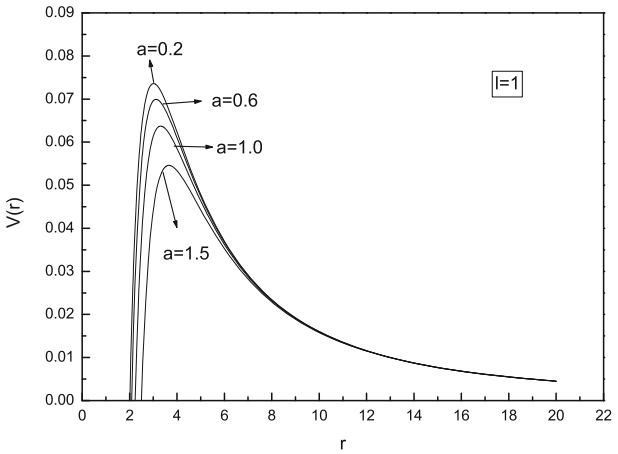

Figure 1. The variation of effective potentials $V(r)$ versus the polar coordinate r for fixed $l = 1$. The lines correspond to the cases with $a = 0.2,\ 0.6,\ 1.0,\ 1.5$, respectively.

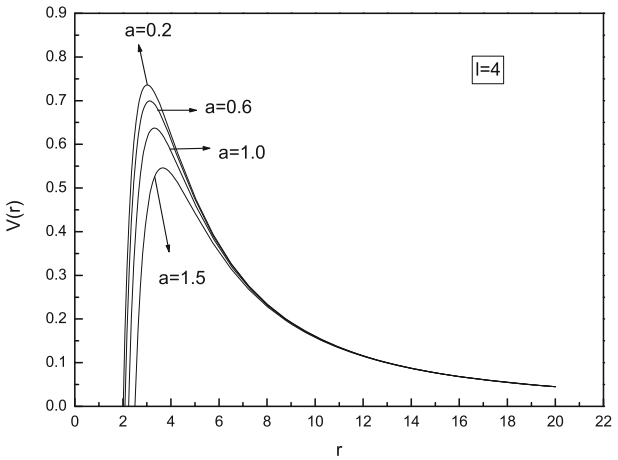

Figure 2. The variation of effective potentials $V(r)$ versus the polar coordinate r for fixed $l = 4$. The lines correspond to the cases with $a = 0.2,\ 0.6,\ 1.0,\ 1.5$, respectively.

hole, and the metric (5) is as in the case of Reissner–Nordström black hole with imaginary electric charge.

From equation (10) we can find that the potential $V(r)$ depends on the quantum correction parameters a and the harmonic angular index l, with $M = 1$, is in the form of a barrier, respectively. This behavior is represented in Figures 1, 2 and 3. Obviously, with the parameters a increasing, the maximum value of potential decrease and the position of peak moves forward to the right side, while both the peak value of the potential barrier and the position of peak increase as l increases.

3. Quasinormal modes frequencies

Equation (9) can be reduced to

$$\frac{\mathrm{d}^2}{\mathrm{d}x^2}\Psi + (\omega^2 - V)\Psi = 0, \tag{11}$$

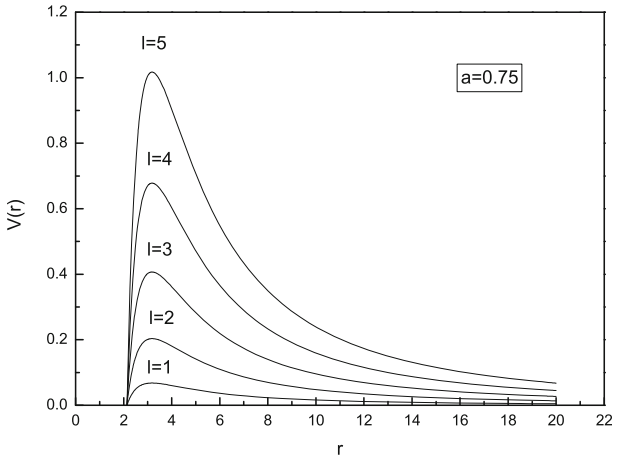

Figure 3. The variation of effective potentials $V(r)$ versus the polar coordinate r for fixed $a = 0.75$. The lines correspond to the cases with $l = 2,\ 3,\ 4,\ 5$, respectively.

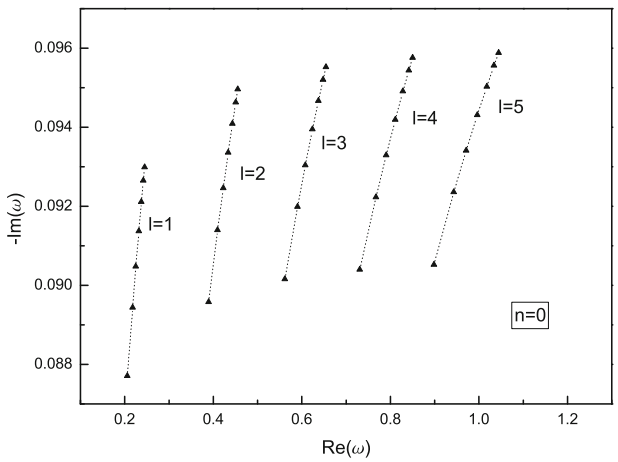

Figure 4. The relation between real parts and magnitudes of imaginary parts of the electromagnetic quasinormal frequencies for the potential $n = 0$.

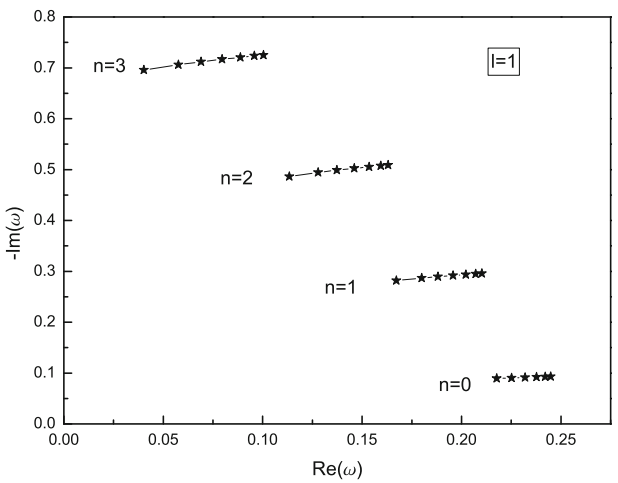

Figure 5. The relation between real parts and magnitudes of imaginary parts of the electromagnetic quasinormal frequencies for the potential $l = 1$.

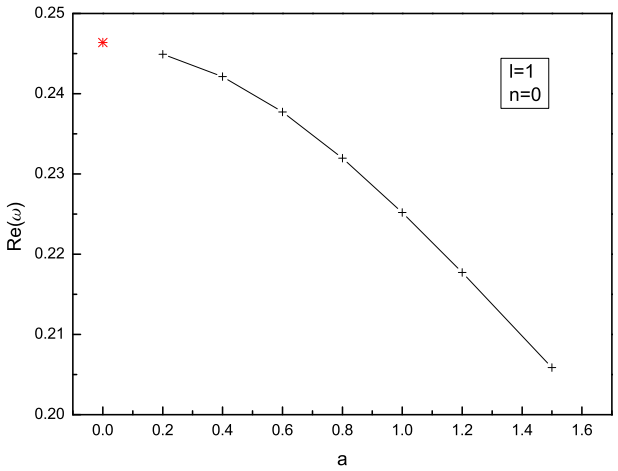

Figure 6. Behavior of the real parts of the electromagnetic quasinormal frequencies with $a = 0.2, 0.4, 0.6, 0.8, 1.0, 1.2, 1.5$ refer to $+$, while $*$ refers to $a = 0$, respectively.

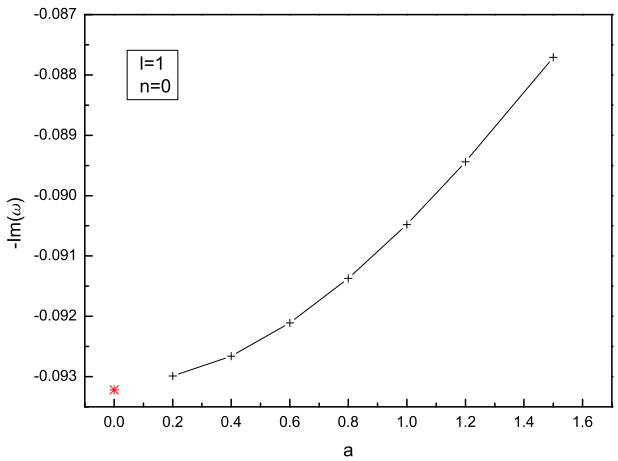

Figure 7. Behavior of the imaginary parts of the electromagnetic quasinormal frequencies with $a = 0.2, 0.4, 0.6, 0.8, 1.0, 1.2, 1.5$ refer to $+$, while $*$ refers to $a = 0$, respectively.

where ω is the complex frequency. The coordinate x is a 'tortoise coordinate' which ranges from $-\infty$ at the horizon to $+\infty$ at the spatial infinity for asymptotically flat spacetime. And the appropriate boundary conditions defining QNMs are purely ingoing waves at the horizon and purely outgoing waves at infinity

$$\Psi(r) \sim \mathrm{e}^{-i\omega x}, \ (x \to -\infty); \quad \Psi(r) \sim \mathrm{e}^{+i\omega x}, \ (x \to +\infty) \tag{12}$$

and only a discrete set of complex frequencies satisfy these conditions.

Let us now study the quasinormal modes of electromagnetic perturbation in the quantum deformation of the Schwarzschild black hole. The numerical results obtained have been given in Appendix. The

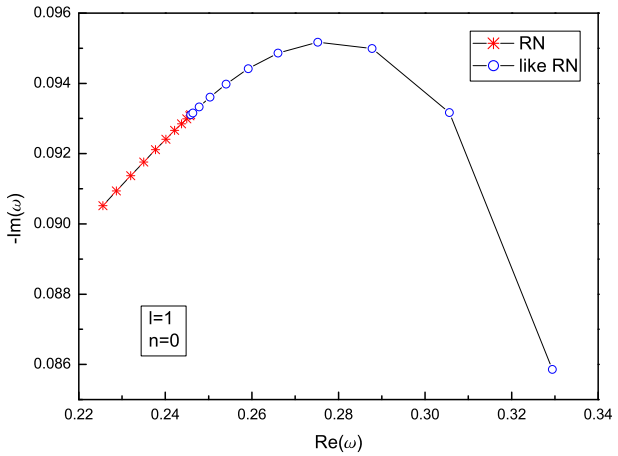

Figure 8. Behavior of the electromagnetic quasinormal frequencies for $l = 1$, $n = 0$. The lines are drawn for Q and a, refers to $0.0, 0.1, 0.2, 0.3, 0.4, 0.5, 0.6, 0.7, 0.8, 0.9, 0.99$, respectively.

data in Table A1 in Appendix is obtained by using WKB method in standard Schwarzschild black hole. In Tables A2–A6 in Appendix, we present the calculation results of quasinormal modes evaluated by the third-order WKB approximation method (Schutz & Will 1985; Iyer & Will 1987; Konoplya 2003), the relationship between the real parts and the magnitudes of imaginary parts of quasinormal frequencies in the background of the black hole are plotted in Figures 4 and 5. The behavior of the real and the imaginary parts of the quasinormal frequencies with varying quantum-correction parameter a are also plotted in Figures 6 and 7. Figure 8 gives the difference behavior of quasinormal modes of electromagnetic perturbation between black hole with imaginary electric charge in equation (5) and standard Reissner–Nordström metric.

4. Conclusion

Using the third-order WKB approximation, we calculated numerically the QNMs frequencies of the electromagnetic perturbation for $M = 1$ with quantum correction of the Schwarzshild black hole. As we all know that the QNMs are characterized by a spectrum of discrete and complex frequencies, whose real parts represent the actual frequency of the oscillation and whose imaginary parts determine the rate at which each mode is damped as a result of the emission of radiation. From these tables and figures, we can obtain the following properties:

(1) The real parts of the quasinormal frequencies as well as the absolute values of imaginary parts of the

quantum corrected Schwarzschild black hole decrease when increasing the quantum correction parameter a, respectively. This phenomenon can be understood from the fact that when a increases, the peak of the effective potential gets higher, the real parts should therefore increase.
(2) With the increase in harmonic angular index l, both the real parts and the magnitudes of the imaginary parts also increase.
(3) The real parts decrease with the overtone number n increase, while the magnitudes of the imaginary parts increase.
(4) From Fig. 8, one can find that the metric (5) coincides with the standard Reissner–Nordström metric but with an imaginary electric charge, which lead to the different behavior of electromagnetic quasinormal frequencies. With an increase in the quantum correction parameter a, both the magnitudes of real and imaginary parts decrease as in Reissner–Nordström with an imaginary electric charge. However, the real parts increase with electric charge Q in the standard Reissner–Nordström, but the magnitudes of imaginary parts increase firstly and then decrease.

Another comparison with the quasinormal modes of electromagnetic perturbations of Schwarzschild black hole without quantum correction (Zhang *et al.* 2007), we can find that the real parts and the magnitudes of the imaginary parts are smaller in the quantum-corrected Schwarzschild black hole. This phenomenon means that the QNMs of electromagnetic perturbations oscillate and damp more slowly. These conclusions will help us understand that the QNMs contain the information of the parameters in a black hole.

In addition, the electromagnetic perturbations around a quantum-corrected Schwarzschild black hole was considered only in this paper, but we did not think about a coupling between the electromagnetic and gravitational perturbations (Sotani *et al.* 2013, 2014), we think that this work will be done in future.

Acknowledgements

This work was supported by the National Natural Science Foundation of China under Grant No. 11147104 and No. 11271055.

Appendix: Numerical results

The numerical results have been given in Tables A1–A6.

Table A1. The quasinormal frequencies of standard Schwarzschild black hole for electromagnetic perturbation ($a = 0$).

l	$\omega(n=0)$	$\omega(n=1)$	$\omega(n=2)$	$\omega(n=3)$
1	0.24639–0.09322i	0.23615–0.29639i	0.20012–0.50331i	0.18676–0.71153i
2	0.45713–0.09507i	0.43583–0.29097i	0.40232–0.49586i	0.36050–0.70564i
3	0.65673–0.09563i	0.64147–0.28980i	0.61511–0.49006i	0.58141–0.69555i
4	0.85301–0.09587i	0.84114–0.28934i	0.81956–0.48700i	0.79094–0.68923i
5	1.04787–0.09598i	1.03815–0.28911i	1.01997–0.48525i	0.99513–0.68511i

Table A2. The quasinormal frequencies of quantum-corrected Schwarzschild black hole for electromagnetic perturbation with $l = 1$.

a	$\omega(n=0)$	$\omega(n=1)$	$\omega(n=2)$	$\omega(n=3)$
0.2	0.24492–0.09299i	0.21024–0.29556i	0.16304–0.50865i	0.10037–0.72506i
0.4	0.24214–0.09266i	0.20710–0.29474i	0.15936–0.50734i	0.09586–0.72340i
0.6	0.23773–0.09211i	0.20215–0.29340i	0.15355–0.50527i	0.08875–0.72066i
0.8	0.23197–0.09137i	0.19572–0.29156i	0.14605–0.50235i	0.07959–0.71684i
1.0	0.22519–0.09048i	0.18822–0.28928i	0.13734–0.49868i	0.06902–0.71199i
1.2	0.21773–0.08944i	0.18003–0.28658i	0.12791–0.49429i	0.05766–0.70615i
1.5	0.20586–0.08771i	0.16724–0.28189i	0.11336–0.48651i	0.04029–0.69570i

Table A3. The quasinormal frequencies of quantum-corrected Schwarzschild black hole for electromagnetic perturbation with $l = 2$.

a	$\omega(n=0)$	$\omega(n=1)$	$\omega(n=2)$	$\omega(n=3)$
0.2	0.45555–0.09496i	0.43416–0.29067i	0.40053–0.49538i	0.35854–0.70499i
0.4	0.45091–0.09463i	0.42929–0.28975i	0.39530–0.49395i	0.35281–0.70305i
0.6	0.44353–0.09409i	0.42156–0.28825i	0.38701–0.49159i	0.34374–0.69985i
0.8	0.43389–0.09336i	0.41145–0.28621i	0.37620–0.48834i	0.33194–0.69543i
1.0	0.42250–0.09246i	0.39955–0.28366i	0.36352–0.48428i	0.31814–0.68988i
1.2	0.40991–0.09140i	0.38642–0.28067i	0.34958–0.47948i	0.30304–0.68329i
1.5	0.38976–0.08958i	0.36551–0.27548i	0.32754–0.47108i	0.27932–0.67170i

Table A4. The quasinormal frequencies of quantum-corrected Schwarzschild black hole for electromagnetic perturbation with $l = 3$.

a	$\omega(n=0)$	$\omega(n=1)$	$\omega(n=2)$	$\omega(n=3)$
0.2	0.65451–0.09552i	0.63919–0.28948i	0.61273–0.48956i	0.57891–0.69487i
0.4	0.64800–0.09520i	0.63251–0.28855i	0.60577–0.48806i	0.57158–0.69284i
0.6	0.63764–0.09467i	0.62189–0.28701i	0.59472–0.48561i	0.55995–0.68951i
0.8	0.62409–0.09395i	0.60801–0.28491i	0.58029–0.48224i	0.54479–0.68492i
1.0	0.60808–0.09304i	0.59162–0.28229i	0.56328–0.47803i	0.52696–0.67916i
1.2	0.59036–0.09199i	0.57350–0.27921i	0.54451–0.47306i	0.50733–0.67235i
1.5	0.56198–0.09016i	0.54454–0.27387i	0.51462–0.46440i	0.47622–0.66042i

Table A5. The quasinormal frequencies of quantum-corrected Schwarzschild black hole for electromagnetic perturbation with $l = 4$.

a	$\omega(n=0)$	$\omega(n=1)$	$\omega(n=2)$	$\omega(n=3)$
0.2	0.85016–0.09576i	0.83823–0.28902i	0.81657–0.48649i	0.78785–0.68853i
0.4	0.84177–0.09544i	0.82972–0.28808i	0.80783–0.48497i	0.77880–0.68646i
0.6	0.82844–0.09491i	0.81618–0.28653i	0.79393–0.48246i	0.76443–0.68304i
0.8	0.81099–0.09419i	0.79847–0.28441i	0.77576–0.47903i	0.74566–0.67835i
1.0	0.79037–0.09329i	0.77755–0.28176i	0.75432–0.47473i	0.72354–0.67248i
1.2	0.76753–0.09223i	0.75440–0.27865i	0.73063–0.46967i	0.69914–0.66553i
1.5	0.73094–0.09040i	0.71734–0.27323i	0.69278–0.46084i	0.66027–0.65339i

Table A6. The quasinormal frequencies of quantum-corrected Schwarzschild black hole for electromagnetic perturbation with $l = 5$.

a	$\omega(n=0)$	$\omega(n=1)$	$\omega(n=2)$	$\omega(n=3)$
0.2	1.04437–0.09588i	1.03461–0.28880i	1.01636–0.48473i	0.99144–0.68440i
0.4	1.03411–0.09556i	1.02425–0.28785i	1.00581–0.48319i	0.98062–0.68229i
0.6	1.01781–0.09503i	1.00778–0.28629i	0.98903–0.48065i	0.96343–0.67882i
0.8	0.99646–0.09431i	0.98621–0.28416i	0.96707–0.47717i	0.94096–0.67406i
1.0	0.97123–0.09341i	0.96074–0.28150i	0.94116–0.47283i	0.91445–0.66809i
1.2	0.94328–0.09236i	0.93253–0.27837i	0.91249–0.46770i	0.88516–0.66105i
1.5	0.89850–0.09052i	0.88737–0.27292i	0.86663–0.45877i	0.83841–0.64875i

References

Berti, E., Cardoso, V., Yoshida, S. 2004, *Phys. Rev. D,* **69**, 124018.

Berti, E., Cardoso, V. 2006, *Phys. Rev. D,* **74**, 104020.

Chandrasekhar, S., Detweiler, S. L. 1975, *Proc. R. Soc. Lond., A* **344**, 441.

Chandrasekhar, S. 1983, in: *The Mathematical Theory of Black Holes.* Oxford University Press, Oxford.

Cardoso, V., Lemos, J. 2001, *Phys. Rev. D,* **64**, 084017; 2003, *Phys. Rev. D,* **67**, 084020.

Chen, S. B., Jing, J. L. 2013, *Phys. Rev. D,* **88**, 064058.

Frolov, V. P., Novikov, I. D. 1998, *Black Hole Physics: Basic Concepts and New Developments*, Kluwer Academic, Dordrecht.

Giammatteo, M., Moss, I. G. 2005, *Class. Quant. Grav.,* **22**, 1803.

Iyer, S., Will, C. M. 1987, *Phys. Rev. D,* **35**, 3621.

Jing, J. L. 2004, *Phys. Rev. D,* **69**, 084009.

Jing, J. L., Pan, Q. Y. 2005, *Phys. Rev. D,* **71**, 124011.

Kokkotas, K. D., Schmidt, B. G. 1999, *Living Rev. Rel.,* **2**, 2.

Kunstatter, G. 2003, *Phys. Rev. Lett.,* **90**, 161301.

Konoplya, R. A. 2002, *Phys. Rev. D* **66**, 044009; 2005, *Phys. Rev. D,* **71**, 024038.

Konoplya, R. A. 2003, *Phys. Rev. D,* 68, 024018.

Kazakov, D. I., Solodukhin, S. N. 1994, *Nucl. Phys. B,* **429**, 153.

Mahamat, S., Bouetou, B. T., Kofane, T. C. 2014, *Astrophys. Space Sci.*, **350**, 721.

Mahamat, S., Bouetou, B. T., Kofane, T. C. 2016, *Astrophys. Space Sci.,* **361**, 137.

Nollert, H. P. 1993, *Phys. Rev. D,* **47**, 5253; 1999, *Class. Quant. Grav.,* **16**, R159.

Regge, T., Wheeler, J. A. 1957, *Phys. Rev.,* **108**, 1063.

Ruffini, R. 1973, in: *Black Holes: les Astres Occlus,* Gordon and Breach Science Publishers.

Schutz, B. F., Will, C. M. 1985, *Astrophys. J. Lett. Ed.,* **291**, 030401.

Shu, F. W., Shen, Y. G. 2004, *Phys. Rev. D,* **70**, 084046.

Sotani, H., Kokkotas, K. D., Laguna, P., Sopuerta, C. F. 2013, *Phys. Rev. D,* **87**, 084018.

Sotani, H., Kokkotas, K. D., Laguna, P., Sopuerta,C. F. 2014, *Gen. Rel. Grav.,* **46**, 1675 .

Vishveshwara, C. V. 1970, *Nature,* **227**, 936.

Wontae, K., Yongwan, K. 2012, *Phys. Lett. B,* **718**, 687.

Zhang, Y., Gui, Y. X., Yu, F., Li, F. L. 2007, *Gen. Relat. Gravit.,* **39**, 1003.